(Amersham, Buckinghamshire, UK). The membrane was incubated with anti-human VASH1 monoclonal antibody (Ab) [5], anti-VEGFR-1 Ab (Santa Cruz Biotechnology, Inc., CA, USA), anti-sVEGFR-1 Ab (Zymed Lab., San Francisco, CA, USA), or anti-ß-actin Ab (Sigma, St. Louis, MO, USA) as the primary antibody according to the manufacturer's instructions. The signal was visualized by using horseradish peroxidase-conjugated secondary antibodies and enhanced chemiluminescence (Immobilon Western, Millipore, Billerica, MA, USA) with a LAS-1000 image analyzer (Fuji Film, Tokyo, Japan).

2.6. Cell Proliferation

Cells were inoculated at a density of 1×10^4 per well into 100 mm dishes, and cultured in 10% FCS/αMEM. After incubation for the desired period, the cells were counted with a hemocytometer.

2.7. Cell Migration

Cells were harvested with trypsin-EDTA, resuspended in 10% FCS/αMEM in a final volume of 100 μL, loaded (5×10^4 cells per well) into the upper chamber of a Transwell Polycarbonate Membrane (pore size: 8 μm; Costar, Cambridge, MA, USA) containing 600 μL of 10% FCS/αMEM in the lower chamber, and incubated at 37 °C for 4 hours. Cells on the lower surface were stained with the reagents from a Diff Quick kit (International Reagents, Kobe, Japan) and counted.

2.8. cDNA Microarray Analysis

Total RNA was isolated from the mock control and clone 4 by ISOGEN according to the manufacturer's instructions. The RNAs were reverse-transcribed in the presence of Cy3 or Cy5-labeled CTP, respectively. The labeled probes were hybridized to a Filgen Array Mouse 32K (Oxford Gene Technology, Oxford, UK) containing 31,769 genes, and the signals were detected by use of a GenePix 4000B (Olympus, Tokyo, Japan). Genes with a Cy5 signal/Cy3 signal ratio >2.0 or < 0.5 were considered to have changed in activity.

2.9. Blood Pressure and Urinary Albumin Excretion of Mice

Animal studies were reviewed and approved by the committee for animal study at our institute in accord with established standards of humane handling. AdVASH1, AdVEGFR-1 or AdLacZ (1×10^9 plaque-forming units [pfu]) was intravenously injected into a tail vein of BALB/c mice (Charles River Laboratories Japan, INC.). Before and seven days after the viral injection, mean blood pressure of conscious mice was measured by the tail cuff method (BP-98A; Softron Co. Ltd., Tokyo, Japan) according to the manufacture's instruction. Seven days after the viral injection, mice were put in mouse metabolic cages (Metabolica type MM; Sugiyama-Gen Iriki Co. Ltd., Tokyo, Japan) and urine was collected for successive eight hour periods. Urine was centrifuged at 2,000× *g* and the urinary albumin level was determined using an ELISA kit (Albuwell M; Exocell, Philadelphia, PA). Urinary creatinine levels were also measured by an ELISA kit (The Creatinine Companion; Exocell).

2.10. Calculations and Statistical Analysis

The statistical significance of differences in the data was evaluated by use of unpaired analysis of variance, and P values were calculated by the unpaired Student t test. $P < 0.05$ was accepted as statistically significant.

3. Results

We introduced the human VASH1 gene into MS1 cells, established bulk transfectants, and thereafter isolated 3 clones. First the expression of VASH1 mRNA and protein was determined (Figure 1A and B). We then examined the properties of the VASH1 expressing mouse endothelial clones. As expected, migration and proliferation were significantly decreased in these VASH1 transfectants (Figures 1C and D).

Figure 1. Establishment of VASH1 overexpressing MS1 clones.

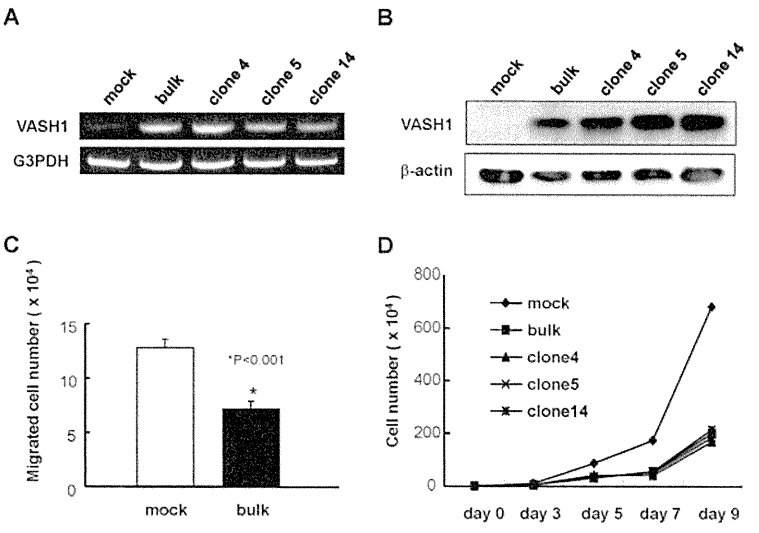

Establishment of VASH1 overexpressing MS1 bulk and clones was described in Materials and Methods. Total RNAs and proteins were extracted from each clone. RT-PCR (A) and Western (B) blot analysis for VASH1 was performed. (C) Migration was compared between mock and VASH1 transfectants. Means and SDs are shown. (D) Proliferation was compared between mock and VASH1 transfectants.

We used clone 4 (Figure 2A) for the following analysis, as it showed the highest expression of VASH1 (Figure 1A). Total RNA was isolated and the gene expression profile was compared with the mock control by cDNA microarray analysis (Figure 2B). The scatter plot of the mock control versus clone 4 is shown in Figure 2B. Among 31,769 mouse genes, 170 genes were increased by more than 200%, whereas 178 genes were decreased by less than 50% in clone 4. The top 20 up-regulated and down-regulated genes are listed in Table 1 and Table 2, respectively. We further evaluated the known angiogenesis-related genes. It was revealed that the expression of 7 genes (CCL2, CCL5, TIMP-1, COX-2, ARNT, CXCL1, and Jagged1) was augmented by more than 200%, whereas that of 2 genes (VEGFR-1 and Ets-1) was down-regulated by less than 50% (Table 3).

Figure 2. Scatter plot of mock vs. VASH1 over expression clone 4.

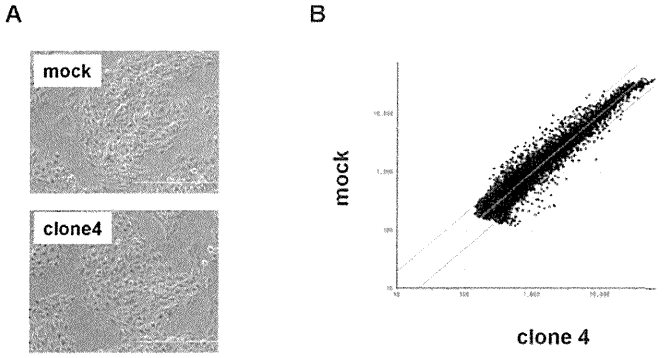

(A) Morphology of mock and VASH1 expressing clone 4 is shown. **(B)** RNAs were extracted from the mock and clone 4, and cDNA microarray analysis was performed as described in Materials and Method. Two lines indicate a 1:2 (lower) or 2:1 (upper) ratio between mock vs. VASH1 overexpressing clone 4.

Table 1. Top 20 up-regulated genes in the VASH1 stable transfectant.

Fold induction	Gene name	Accession No.
8.07	Estradiol 17 beta-dehydrogenase 5	NM_030611
7.65	T-cell specific GTPase	NM_011579
6.16	Dematin	NM_013514
5.43	interferon-induced protein with tetratricopeptide repeats 3	NM_010501
4.91	Osteoactivin	NM_053110
4.63	BTB/POZ domain containing protein 9	NM_172618
4.29	interferon, alpha-inducible protein	NM_172618
4.26	Galectin-3	NM_010705
4.19	ADP-ribosylation factor-like 2 binding protein	NM_024191
3.79	potassium channel interacting protein 4	NM_030265
3.79	CCL2	NM_011333
3.78	olfactory receptor 576	NM_001001805
3.59	KELCH-like protein 4	NM_172781
3.41	interferon-induced protein 44	NM_133871
3.39	interferon, alpha-inducible protein 27	NM_029803
3.12	acyl-Coenzyme A thioesterase 2	NM_019736
3.28	stefin A2 like 1	NM_173869
3.11	guanylate nucleotide binding protein 3	NM_018734
3.09	2'-5'-oligoadenylate synthetase 1A	NM_145211
3.00	Male-specific lethal 3-like 1	NM_010832

Table 2. Top 20 down-regulated genes in the VASH1 stable transfectant.

Fold induction	Gene name	Accession No.
0.22	Phospholipid transfer protein	NM_011125
0.22	VEGFR1	NM_010228
0.28	Oligodendrocyte transcription factor 1	NM_016968
0.28	olfactory receptor 635	NM_147118

Table 2. *Cont.*

0.28	PHD finger protein 19	NM_028716
0.28	Trace amine receptor 1	NM_053205
0.29	Gastrokine 1	NM_025466
0.29	Mast cell carboxypeptidase A	NM_007753
0.30	poliovirus receptor-related 2	NM_008990
0.30	Versican core protein	XM_488510
0.30	Janus kinase 3	NM_010589
0.30	thrombopoietin	NM_009379
0.31	nudix	NM_025539
0.31	Anaplastic lymphoma kinase	NM_007439
0.33	Lymphocyte antigen 86	NM_010745
0.33	Fc receptor-like 3	NM_144559
0.34	Serine/threonine-protein kinase ULK1	NM_009469
0.34	Runt-related transcription factor 3	NM_019732
0.34	RAB GTPase activating protein 1	AK_044346
0.35	kidney expressed gene 1	NM_029550

Table 3. Altered expression of angiogenesis-related genes in the VASH1 transfectant.

Gene name	**Fold induction**
VEGFR1	0.22
Ets-1	0.45
Jagged1	2.06
CXCL1	2.17
ARNT	2.18
COX-2	2.38
TIMP-1	2.39
CCL5	2.45
CCL2	3.79

Here we focused our attention on VEGFR-1, the most down-regulated gene. The characteristic feature of the VEGFR-1 gene is that it encodes not only a full-length membrane receptor but also a soluble form (sVEGFR-1) carrying the VEGF-binding domain as well as a 31-amino-acid stretch derived from an intron [22]. We therefore analyzed the expression of sVEGFR-1 as well. RT-PCR and Western blot analyses showed decrease expression of VEGFR-1 and sVEGFR-1 in all VASH1 expressing clones (Figures 3A and 3B). To further confirm these results, we transiently overexpressed VASH1 in HUVECs. RT-PCR and Western blot analyses also showed this decrease in the levels of VEGFR-1 and sVEGFR-1 (Figures 3C and D).

sVEGFR-1 is a decoy receptor and inhibits VEGF mediated signals. VASH1 is a VEGF-inducible angiogenesis inhibitor expressed in ECs. We therefore examined whether sVEGFR-1 affects the expression of VASH1 in ECs. To do so, we transiently overexpressed the sVEGFR-1 gene in HUVECs. RT-PCR and Western blot analyses demonstrated that sVEGFR-1 down-regulated the expression of VASH1 in HUVECs (Figure 4).

Figure 3. VASH1 inhibits VEGFR-1 and sVEGFR-1 expression in ECs.

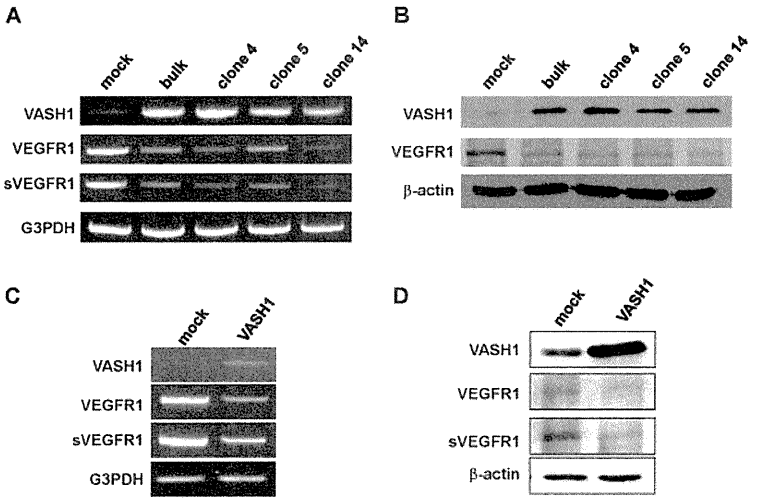

Total RNAs and proteins were extracted from mock cells and from each VASH1 overexpressing clone, and RT-PCR (A) and Western blot analysis (B) for VEGFR-1 and sVEGFR-1 were performed as described in Materials and Method. The HUVECs were infected with the Lac-Z or VASH1 adenovirus vector at a multiplicity of infection (MOI) of 30. After the infection, total RNAs and proteins were extracted from vasohibin-1 over expression HUVECs. RT-PCR (C) and Western (D) blot analysis for VEGFR-1 and sVEGFR-1 was performed.

Figure 4. sVEGFR-1 inhibits VASH1 expression in ECs.

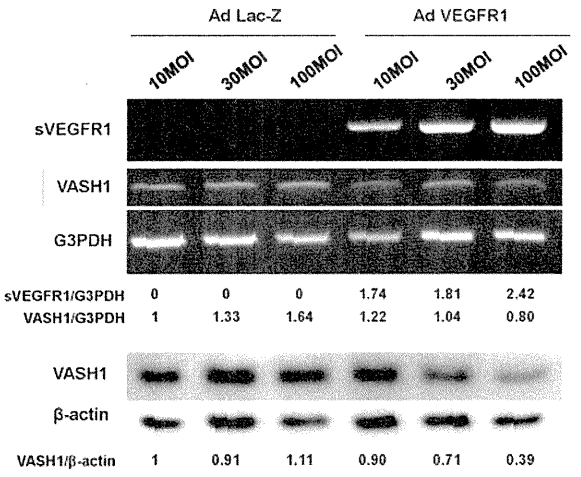

The HUVECs were infected with the AdsVEGFR-1 at the indicated a multiplicity of infection (MOIs). After the infection, total RNAs and proteins were extracted from sVEGFR-1 overexpressing HUVECs. RT-PCR (upper panel) and Western blot analysis (lower panel) for VASH1 were performed. Intensity of bands was quantified, and standardized values are shown.

The blockade of VEGF mediated signals causes regression of normal quiescent vessels, hypertension and proteinuria [21]. Here we examined whether VASH1 caused hypertension and proteinuria. AdsVEGFR-1 increased mean blood pressure, but AdVASH1 did not (Figure 5A). Similarly AdsVEGFR-1 increased the urinary albumin excretion, but AdVASH1 did not (Figure 5B).

AdVASH1 exhibited little effect on the increased mean blood pressure or urinary albumin excretion induced by AdsVEGFR-1 (Figure 5 A and B).

Figure 5. Different effects of sVEGFR-1 and VASH1 on blood pressure and urinary albumin excretion.

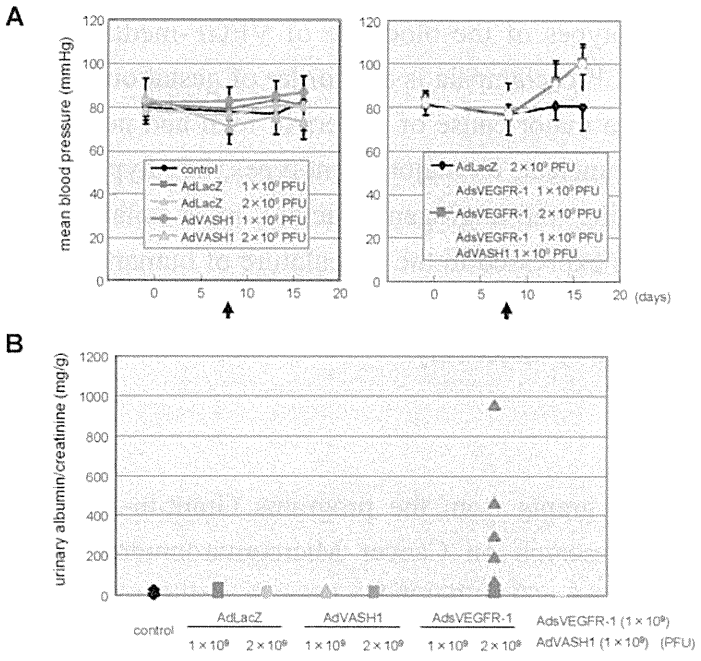

A: Indicated PFU of adenovirus vectors were injected *via* a tail vain on day 8. Arrows indicate the timing of adenovirus injection. Mean blood pressure was assessed on day 0, 7, 12, 16; means and SDs are shown. **B**: Indicated PFU of adenovirus vectors were injected. Twenty-four-hour urinary albumin excretion was quantified on day 7 after the adenovirus injection.

4. Discussion

Here we analyzed the target genes of VASH1 in ECs, and revealed for the first time that VASH1 down-regulated the expression of both full-length and soluble form of VEGFR-1 in ECs. Interestingly, sVEGFR-1, a decoy receptor that blocks VEGF mediated signals, down-regulated the expression of VASH1 in return. Endogenous sVEGFR-1 is thought to inhibit angiogenesis by reducing VEGF-mediated angiogenic signals [22]. Thus, our present study indicates that these two factors mutually regulate their expression in ECs. We propose that VASH1 and sVEGFR-1 interact with each other within ECs for the fine tuning of angiogenesis.

The expression of VASH1 in ECs is known to be induced by VEGF-VEGFR2 and its downstream PKC-δ mediated signaling pathway [6]. We therefore think it reasonable that sVEGFR-1 would inhibit the expression of VASH1 in ECs. In contrast, the regulation of the expression of full-length and soluble form of VEGFR-1 is not well characterized. Further study is required to elucidate the mechanism as to how VASH1 down-regulates the expression of VEGFR-1 in ECs.

From the clinical experience of anti-angiogenic cancer treatment, it is now well recognized that the *in vivo* blockade of VEGF-mediated signals causes vascular complications including hypertension and proteinuria [21]. Indeed, the tail vein injection of AdsVEGFR-1 increased blood pressure and induced

proteinuria (Figure 5). In contrast to the blockade of VEGF-mediated signals, we recently reported that VASH1 did not cause any vascular regression [23]. Here we extended our analysis on the vascular complication, and demonstrated that VASH1 did not cause hypertension or proteinuria. VASH1 could not prevent the hypertension or proteinuria induced by sVEGFR-1. Nevertheless, this finding that VASH1 caused neither hypertension nor proteinuria can be a merit of VASH1 when this inhibitor is applied as anti-angiogenic treatment.

In relation to vascular phenotypes of the blockade of VEGF-mediated signals, much attention is now being paid to preeclampsia. Preeclampsia is a disorder of gestation characterized by hypertension and renal dysfunction, and it is a major cause of maternal, fetal and neonatal mortality. Although the etiology of preeclampsia is still unclear, its major phenotypes, i.e., hypertension and proteinuria, may be due to an excess of circulating anti-angiogenic factors, most notably sVEGFR-1 [24]. We have previously shown that VASH1 is expressed in the vasculature of human placenta [6]. In this context, it would be interesting to examine the significance of VASH1 in normal pregnancy and patients with preeclampsia. Such study is currently under way.

Acknowledgements

This work was supported by grants from the programs Grant-in-Aid for Scientific Research on Innovative Areas "Integrative Research on Cancer Microenvironment Network" (22112006) and a Grant-in-Aid for Scientific Research (C) (22590821) from the Ministry of Education, Culture, Sports, Science, and Technology of Japan, and by Health and Labour Sciences research grants, Third Term Comprehensive Control Research for Cancer, from the Ministry of Health, Labour and Welfare of Japan.

References

1. Sato, Y. Update on endogenous inhibitors of angiogenesis. *Endothelium* **2006**, *13*, 147-155.
2. Ferrara, N. Vascular endothelial growth factor. *Arterioscler. Thromb. Vasc. Biol.* **2009**, *29*, 789-791.
3. Fong, G.H.; Rossant, J.; Gertsenstein, M.; Breitman, M.L. Role of the Flt-1 receptor tyrosine kinase in regulating the assembly of vascular endothelium. *Nature* **1955**, *376*, 66-70.
4. Hiratsuka, S.; Minowa, O.; Kuno, J.; Noda, T.; Shibuya, M. Flt-1 lacking the tyrosine kinase domain is sufficient for normal development and angiogenesis in mice. *Proc. Natl. Acad. Sci. USA* **1998**, *95*, 9349-9354.
5. Watanabe, K.; Hasegawa, Y.; Yamashita, H.; Shimizu, K.; Ding, Y.; Abe, M.; Ohta, H.; Imagawa, K.; Hojo, K.; Maki, H.; *et al.* Vasohibin as an endothelium-derived negative feedback regulator of angiogenesis. *J. Clin. Invest.* **2004**, *114*, 898-907.
6. Shimizu, K.; Watanabe, K.; Yamashita, H.; Abe, M.; Yoshimatsu, H.; Ohta, H.; Sonoda, H.; ;Sato, Y. Gene regulation of a novel angiogenesis inhibitor, vasohibin, in endothelial cells. *Biochem. Biophys. Res. Commun.* **2005**, *327*, 700-706.
7. Shibuya, T.; Watanabe, K.; Yamashita, H.; Shimizu, K.; Miyashita, H.; Abe, M.; Moriya, T.; Ohta, H.; Sonoda, H.; Shimosegawa, T.; *et al.* Isolation and characterization of vasohibin-2 as a homologue of VEGF-inducible endothelium-derived angiogenesis inhibitor vasohibin. *Arterioscler. Thromb. Vasc. Biol.* **2006**, *26*, 1051-1057.

8. Kimura, H.; Miyashita, H.; Suzuki, Y.; Kobayashi, M.; Watanabe, K.; Sonoda, H.; Ohta, H.; Fujiwara, T.; Shimosegawa, T.; Sato, Y. Distinctive localization and opposed roles of vasohibin-1 and vasohibin-2 in the regulation of angiogenesis. *Blood* **2009**, *113*, 4810-4818.
9. Hosaka, T.; Kimura, H.; Heishi, T.; Suzuki, Y.; Miyashita, H.; Ohta, H.; Sonoda, H.; Moriya, T.; Suzuki, S.; Kondo, T.; *et al.* Vasohibin-1 expressed in endothelium of tumor vessels regulates angiogenesis. *Am. J. Pathol.* **2009**, *175*, 430-439.
10. Yoshinaga, K.; Ito, K.; Moriya, T.; Nagase, S.; Takano, T.; Niikura, H.; Yaegashi, N.; Sato, Y. Expression of vasohibin as a novel endothelium-derived angiogenesis inhibitor in endometrial cancer. *Cancer Sci.* **2008**, *99*, 914-919.
11. Tamaki, K.; Moriya, T.; Sato, Y.; Ishida, T.; Maruo, Y.; Yoshinaga, K.; Ohuchi, N.; Sasano, H. Vasohibin-1 in human breast carcinoma: a potential negative feedback regulator of angiogenesis. *Cancer Sci.* **2008**, *100*, 88-94.
12. Tamaki, K.; Sasano, H.; Maruo, Y.; Takahashi, Y.; Miyashita, M.; Moriya, T.; Sato, Y.; Hirakawa, H.; Tamaki, N.; Watanabe, M.; *et al.* Vasohibin-1 as a potential predictor of aggressive behavior of ductal carcinoma *in situ* of the breast. *Cancer Sci.* **2010**, *101*, 1051-1058.
13. Yoshinaga, K.; Ito, K.; Moriya, T.; Nagase, S.; Takano, T.; Niikura, H.; Sasano, H.; Yaegashi, N.; Sato, Y. Roles of intrinsic angiogenesis inhibitor, vasohibin, in cervical carcinomas. *Cancer Sci.* **2011**, *102*, 446-451.
14. Yamashita, H.; Abe, M.; Watanabe, K.; Shimizu, K.; Moriya, T.; Sato, A.; Satomi, S.; Ohta, H.; Sonoda, H.; Sato, Y. Vasohibin prevents arterial neointimal formation through angiogenesis inhibition. *Biochem. Biophys. Res. Commun.* **2006**, *345*, 919-925.
15. Wakusawa, R.; Abe, T.; Sato, H.; Yoshida, M.; Kunikata, H.; Sato, Y.; Nishida, K. Expression of vasohibin, an antiangiogenic factor, in human choroidal neovascular membranes. *Am. J. Ophthalmol.* **2008**, *146*, 235-243.
16. Sato, H.; Abe, T.; Wakusawa, R.; Asai, N.; Kunikata, H.; Ohta, H.; Sonoda, H.; Sato, Y.; Nishida, K. Vitreous levels of vasohibin-1 and vascular endothelial growth factor in patients with proliferative diabetic retinopathy. *Diabetologia* **2009**, *52*, 359-361.
17. Shen, J.; Yang, X.; Xiao, W.H.; Hackett, S.F.; Sato, Y.; Campochiaro, P.A. Vasohibin is up-regulated by VEGF in the retina and suppresses VEGF receptor 2 and retinal neovascularization. *FASEB J.* **2006**, *20*, 723-725.
18. Arbiser, J.L.; Moses, M.A.; Fernandez, C.A.; Ghiso, N.; Cao, Y.; Klauber, N.; Frank, D.; Brownlee, M.; Flynn, E.; Parangi, S.; *et al.* Oncogenic H-Ras stimulates tumor angiogenesis by two distinct pathways. *Proc. Natl. Acad. Sci. USA* **1997**, *94*, 861-866.
19. Novak, A.; Guo, C.; Yang, W.; Nagy, A.; Lobe, C.G. Z/EG, a double reporter mouse line that expresses enhanced green fluorescent protein upon Cre-mediated excision. *Genesis* **2000**, *28*, 147-155.
20. Namba, K.; Abe, M.; Saito, S.; Satake, M.; Ohmoto, T.; Watanabe, T.; Sato, Y. Indispensable role of the transcription factor PEBP2/CBF in angiogenic activity of a murine endothelial cell MSS31. *Oncogene* **2000**, *19*, 106-114.
21. Roodhart, J.M.; Langenberg, M.H.; Witteveen, E.; Voest, E.E. The molecular basis of class side effects due to treatment with inhibitors of the VEGF/VEGFR pathway. *Curr. Clin. Pharmacol.* **2008**, *3*, 132-143.

22. Lamszus, K.; Ulbricht, U.; Matschke, J.; Brockmann, M.A.; Fillbrandt, R.; Westphal, M. Levels of soluble vascular endothelial growth factor (VEGF) receptor 1 in astrocytic tumors and its relation to malignancy, vascularity, and VEGF-A. *Clin. Cancer Res.* **2003**, *9*, 1399-1405.
23. Heishi, T.; Hosaka, T.; Suzuki, Y.; Miyashita, H.; Oike, Y.; Takahashi, T.; Nakamura, T.; Arioka, S.; Mitsuda, Y.; Takakura, T.; *et al.* Endogenous angiogenesis inhibitor vasohibin1 exhibits broad-spectrum antilymphangiogenic activity and suppresses lymph node metastasis. *Am. J. Pathol.* **2010**, *176*, 1950-1958.
24. Mutter, W.P.; Karumanchi, S.A. Molecular mechanisms of preeclampsia. *Microvasc. Res.* **2008**, *75*, 1-8.

Vascular Pharmacology 56 (2012) 262–266

Contents lists available at SciVerse ScienceDirect

Vascular Pharmacology

journal homepage: www.elsevier.com/locate/vph

Review

The vasohibin family: Novel regulators of angiogenesis

Yasufumi Sato *

Department of Vascular Biology, Institute of Development, Aging and Cancer, Tohoku University, 4-1 Seiryo-machi, Aoba-ku, Sendai 980-8575, Japan

ARTICLE INFO

Article history:
Received 15 November 2011
Received in revised form 5 January 2012
Accepted 15 January 2012

Keywords:
Vasohibin
Angiogenesis

ABSTRACT

Angiogenesis is thought to be regulated by the local balance between angiogenesis stimulators and angiogenesis inhibitors. A number of endogenous regulators of angiogenesis have been found in the body. We recently isolated vasohibin-1 (VASH1) as a negative feedback regulator of angiogenesis produced by endothelial cells, and VASH2 as a homologue of VASH1 thereafter. We found that VASH1 was expressed in endothelial cells to terminate angiogenesis, whereas VASH2 promoted angiogenesis, in the mouse model of angiogenesis. This mini-review will focus on the vasohibin family in relation to the regulation of angiogenesis.

Contents

1. Introduction

The vasculature is primarily composed of luminal endothelial cells (ECs) and surrounding mural cells (smooth muscle cells or pericytes). ECs are multifunctional cells covering the entire luminal surface of all blood vessels. They form an interface between the circulating blood in the lumen and the rest of the vessel wall, and maintain vascular homeostasis. ECs control the transport of various molecules across the vascular wall, regulate the adhesion of leukocytes for extravasation, manipulate vascular tonus, and prevent thrombotic events. When stimulated by angiogenic factors, ECs form neo-vessels. The initial step of angiogenesis is the extrication of mural cells from the endothelial tubes for vascular destabilization. Subsequently, specialized ECs, the so-called "tip" cells, migrate by extending numerous filopodia, whereas the ECs that follow them, the so-called "stalk" cells, proliferate, causing elongation of the sprouts to form immature tube-like structures. Finally, redistributed mural cells affix themselves to the newly formed vessels for vascular restabilization. By this process, ECs stop their proliferation, thus terminating angiogenesis (Gerhardt and Betsholtz, 2003).

The body contains a number of endogenous angiogenesis stimulators and inhibitors, and the local balance between them regulates this process of blood vessel formation. Angiogenesis stimulators are mostly growth factors and cytokines including vascular endothelial growth factor (VEGF), whereas angiogenesis inhibitors are variable and include hormones, chemokines, proteins accumulated in the extracellular matrix, proteolytic fragments of various proteins, and so forth (Sato, 2006). In addition, the majority of angiogenesis inhibitors are extrinsic to the vasculature; however, some are constitutively expressed there and act as barriers to prevent the invasion by sprouts, and other factors are generated in response to certain stimuli and counteract this process. Recently, however, ECs themselves have been found to produce intrinsic angiogenesis inhibitors. Such inhibitors may regulate angiogenesis in an auto-regulatory or negative-feedback fashion.

2. Vasohibin-1 (VASH1)

We hypothesized that ECs themselves might produce either positive or negative regulators of angiogenesis. To test this hypothesis, we

* Tel.: +81 22 717 8528; fax: +81 22 717 8533.
E-mail address: y-sato@idac.tohoku.ac.jp.

1537-1891/$ – see front matter © 2012 Elsevier Inc. All rights reserved.
doi:10.1016/j.vph.2012.01.002

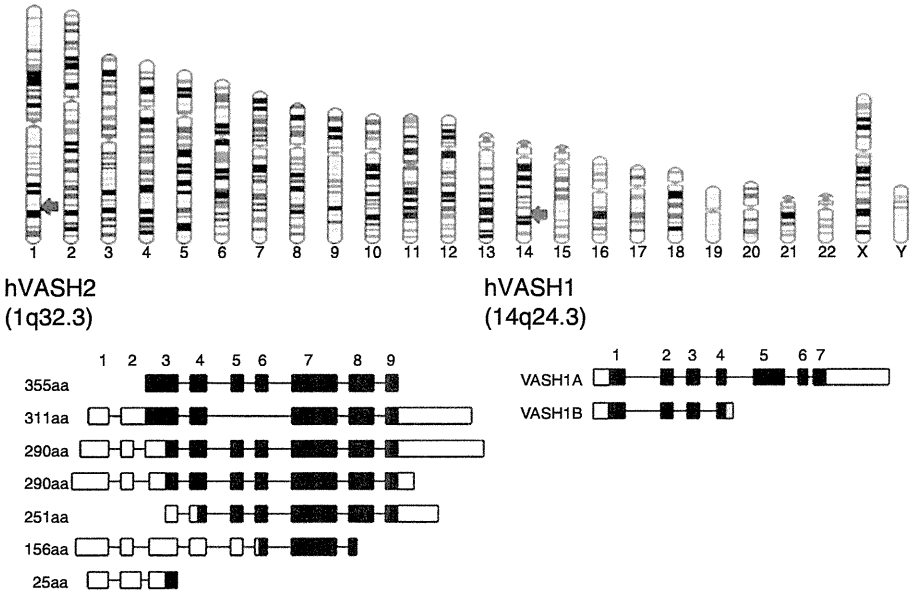

Fig. 1. *VASH1* and *VASH2* genes and their transcripts.The human *VASH1* gene is encoded in 14q24.3; and the human *VASH2* gene, in 1q32.3. There are multiple transcripts in both human VASH1 and VASH2. Black squares indicate the exons encoding the protein.

performed DNA microarray analysis to detect VEGF-inducible genes in ECs (Abe and Sato, 2001). Among a variety of VEGF-inducible genes, we focused our attention on those genes whose functions were undefined at that time. We performed *in vitro* functional assays for angiogenesis, isolated the molecule VASH1, and demonstrated its anti-angiogenic activity *in vivo* (Watanabe et al., 2004). The gene for human *VASH1* gene is located on chromosome 14q24.3, and consists of 7 exons (Fig. 1). There are 2 isoforms of human VASH1: full-length VASH1A and its spliced variant, VASH1B (Fig. 1). Human VASH1A protein is composed of 365 amino acid residues; whereas human VASH1B protein is composed of 204 amino acid residues, and this splicing variant also has the anti-angiogenic activity (Shimizu et al., 2005; Kern et al., 2008).

The VEGFR-induced expression of VASH1 in ECs is mediated via VEGFR2 and its downstream effector PKCδ (Shimizu et al., 2005). VASH1 is induced not only by VEGF but also by fibroblast growth factor 2 (FGF-2), another potent angiogenic factor (Watanabe et al., 2004; Shimizu et al., 2005); and this induction is also mediated by PKCδ (Shimizu et al., 2005). Accordingly, the principal signaling pathways for the induction of VASH1 by these 2 representative angiogenic growth factors considerably overlap. Interestingly, this induction of VASH1 in ECs disappears under a hypoxic condition or in the presence of inflammatory cytokines such as TNFα and IL-1 (Shimizu et al., 2005).

Immunohistochemical analysis revealed that VASH1 protein is present in ECs in the developing human or mouse embryo, but is reduced in expression in the post-neonate (Shibuya et al., 2006). Nimmagadda et al. independently showed by *in situ* hybridization that VASH1 mRNA is expressed in a wide range of tissues and organs in the chicken embryo, and suggested that the expression of VASH1 might not be limited to ECs (Nimmagadda et al., 2007). Indeed, we could detect VASH1 mRNA in hematopoietic stem cells in the bone marrow (Naito et al., 2009). Nevertheless, our immunohistochemical analysis preferentially detected VASH1 protein in ECs at the site of angiogenesis (Watanabe et al., 2004; Shibuya et al., 2006). We further investigated the expression of VASH1 under various conditions giving rise to pathological angiogenesis. The presence of VASH1 in ECs is evident in various cancers, atherosclerotic lesions, age-dependent macular degeneration (AMD), diabetic retinopathy, and rheumatoid arthritis (Yamashita et al., 2006; Yoshinaga et al., 2008; Wakusawa et al., 2008; Tamaki et al., 2008; Sato et al., 2009; Hosaka et al., 2009; Miyake et al., 2009; Tamaki et al., 2010; Yoshinaga et al., 2011). Even under these pathological conditions, the extent of angiogenesis may vary in its natural course. Interestingly, patients with active AMD tend to have a lower VASH1-to-VEGF mRNA ratio than those with the inactive disease (Wakusawa et al., 2008). Tumors inoculated into *VASH1 (−/−)* mice contain numerous immature vessels, resulting in a growth advantage to the tumors (Hosaka et al., 2009). These observations suggest that VASH1 may regulate the course of angiogenesis under pathological conditions as well.

Peripheral lymphatic vessels are composed of a single layer of lymphatic ECs without mural cell coverage, and their function is to collect fluid lost from blood vessels and to maintain immune responses, lipid uptake, and tissue homeostasis. Recently, attention has been focused on lymphangiogenesis, which is the formation of new lymphatic vessels; because it has been shown to be related to the lymph node (LN) metastasis of cancers. Angiogenesis is counter-balanced by various endogenous inhibitors. However, little is known about endogenous inhibitors of lymphangiogenesis. We reevaluated the effect of VASH1 by using the corneal micropocket assay, and observed its broad-spectrum anti-angiogenic as well as anti-lymphangiogenic activities (Heishi et al., 2010). In addition, we found that VASH1 inhibits tumor lymphangiogenesis and tumor LN metastasis (Heishi et al., 2010). To our knowledge, VASH1 is the first molecule intrinsic to the endothelium that exhibits anti-lymphangiogenic activities.

3. Vasohibin-2 (VASH2)

By database searching, we found 1 gene homologous to *VASH1*, and designated it as *VASH2* (Nimmagadda et al., 2007). The gene for human *VASH2* is located on chromosome 1q32.3. So far, the 9 exons for the *VASH2* gene have been shown in the database to form multiple transcripts owing to alternative splicing (Fig. 1). We found that full-length human VASH2, composed of 355 amino acid residues, was expressed in cultured ECs (Nimmagadda et al., 2007). The expression of VASH2 seems to be constitutive and cannot be induced by any growth factors or cytokines.

Because of the similarity between VASH1 and VASH2, we examined their spatiotemporal expression and function during angiogenesis (Kimura et al., 2009). Our analysis using the mouse subcutaneous angiogenesis model revealed that VASH1 is expressed not in ECs at the sprouting front but in newly formed blood vessels behind the sprouting front where angiogenesis is terminated. In contrast, VASH2

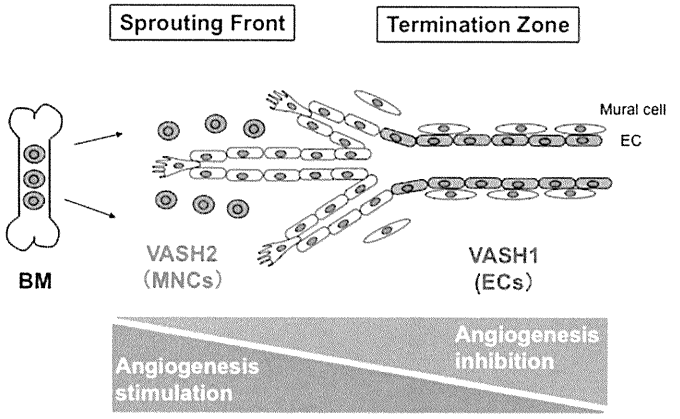

Fig. 2. Spatial expression and function of VASH1 and VASH2 in the regulation of angiogenesis.VASH1 is mainly expressed in ECs at the termination zone and halts angiogenesis. In contrast, VASH2 is mainly expressed in MNCs at the sprouting front and promotes angiogenesis. BM: bone marrow.

is expressed preferentially in mononuclear cells (MNCs) that are mobilized from the bone marrow and infiltrate the sprouting front. We then generated VASH1 and VASH2 knockout mice. *VASH1 KO* mice contain numerous immature microvessels in the area where angiogenesis should be terminated. This phenotype is gene-dosage sensitive, as angiogenesis is greater in *VASH1 (−/−)* mice than in *VASH1 (+/−)* ones (Kimura et al., 2009). Importantly, newly formed immature microvessels in *VASH1 (−/−)* mice are functional, as indicated by blood flow (Kimura et al., 2009). In contrast, *VASH2 KO* mice contain fewer neovessels in the sprouting front of angiogenesis. This phenotype is also gene-dosage sensitive, as more impaired angiogenesis is observed in the *VASH2 (−/−)* mice (Kimura et al., 2009). Importantly, the degree of infiltration of the sprouting front by MNCs in *VASH2 (−/−)* mice is identical to that in wild-type mice (Kimura et al., 2009). As stated above, the expression of VASH1 is low in proliferating ECs at the sprouting front, but is high in non-proliferating ECs (Kimura et al., 2009). In addition, angiogenesis in the *VASH2* knockout mice is deficient at the sprouting front (Kimura et al., 2009). These results indicate that VASH1 is expressed in ECs in the termination zone of angiogenesis to terminate angiogenesis and that VASH2 is mainly expressed in MNCs in the sprouting front and promotes angiogenesis (Fig. 2).

4. Small vasohibin-binding protein (SVBP)

To disclose the undefined characteristics of vasohibins, we searched for their possible binding partners by using the yeast two-hybrid technique and discovered 1 candidate gene (Suzuki et al., 2010). This gene has been registered as hypothetical protein LOC374969 or coiled-coil domain containing 23. We confirmed the binding of this protein to VASH1 and VASH2 by using the BIAcore system (Fig. 3). Since this protein is composed of only 66 amino acids, we renamed it as SVBP (Suzuki et al., 2010). A database search revealed that SVBP is highly conserved among species (Fig. 3). We then examined the function of SVBP and found that this small molecule binds to vasohibins within the cell, forming a hetero-complex and facilitating the secretion of vasohibin from the cell. As vasohibins lack the classical signal sequence for secretion, it has been unclear whether vasohibins are indeed secreted (Suzuki et al., 2010). We therefore propose that SVBP functions as a secretory chaperone of vasohibins.

5. Bioinformatics of VASH1 and VASH2

The overall homology between full-length human VASH1 and VASH2 is 52.5% at the amino acid level. We conducted a database search on VASH1 and VASH2 of different species and discovered that the sea squirt possesses 1 common ancestral vasohibin gene and that the homology between this ancestral gene and human VASH1 or human VASH2 is almost the same. All vertebrates have VASH1 and VASH2. Thus, this common ancestral gene seems to be have divided into VASH1 and VASH2 during the evolution to vertebrate. Amino acid sequences of mammalian VASH1 and VASH2 are well conserved among species, and this trend is more noticeable for VASH2 (Fig. 4).

We searched for known functional motifs in the amino acid sequences, but we could not find any in either VASH1 or VASH2, making it extremely difficult to estimate and compare the functions or three-dimensional structures of these 2 molecules. We therefore surveyed the order/disorder orientation of VASH1 and VASH2 proteins. The order region defines stability in a three-dimensional composition whereas the disorder region defines instability in it. As shown in Fig. 5, VASH1 and VASH2 contain disorder regions (in red type) in both N-terminus and C-terminus ends, with order regions (in black type) in the middle part of their structure. The overall order/disorder probability lines of VASH1 and VASH2 considerably resemble each

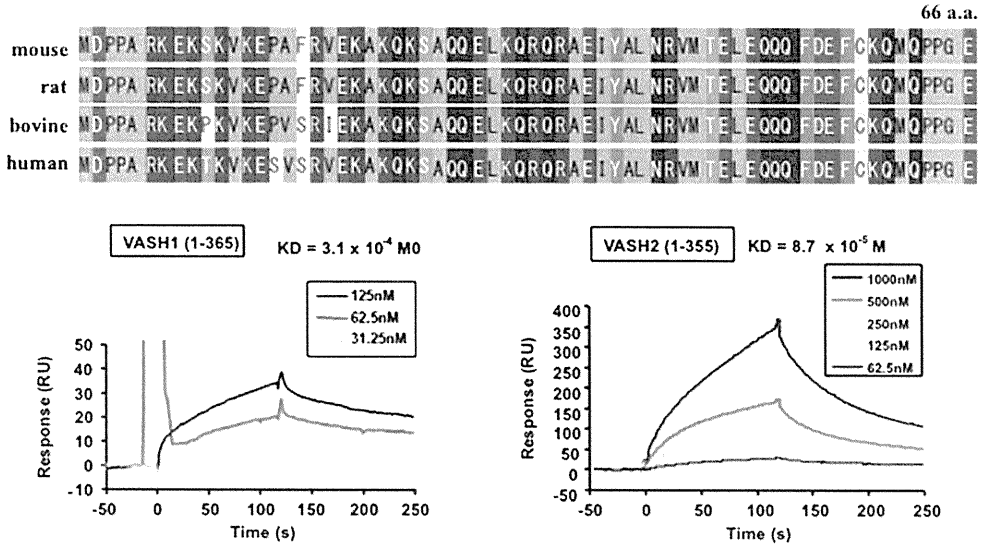

Fig. 3. SVBP of various species and its binding to VASH1/VASH2.Amino acid sequences of SVBP from the indicated species are shown in the upper panel. Binding characteristics of SVAB and VASH1/VASH2 are seen in the lower panel.

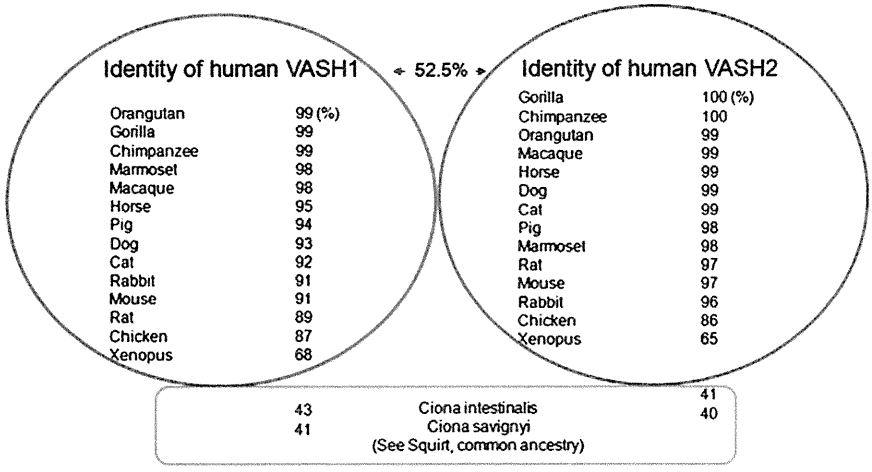

Fig. 4. Vasohibin family proteins of various species.Similarities of vasohibin family proteins of various species are shown. Proteins within the red circle are VASH1; and those within the blue circle, VASH2. Proteins within the green rectangle are ancestral gene products.

other, indicating the correspondence of these 2 molecules. However, when the similarity of order and disorder areas of the VASH's is compared, the resemblance in the disorder areas is less (Fig. 5). As it has been recently noted, the disorder region is more important than the order one for determining the function of proteins (Uversky, 2011). Therefore, differences in the disorder regions may indicate the distinctive function of VASH1 and VASH2.

6. Concluding remarks

The present mini-review has focused on the novel VASH family of proteins, VASH1 and VASH2. VASH1 and VASH2 are highly conserved among species. However, the lack of any known functional motifs makes it extremely difficult to estimate and compare the functions or three-dimensional structures of VASH1 and VAH2. Nevertheless, our analysis indicates that their roles in the regulation of angiogenesis are distinct and perhaps contradictory.

We are now characterizing their receptor and its downstream signaling. We hope that our work will disclose the entire function of this unique family of proteins.

Acknowledgements

I thank Professor Kengo Kinoshita at Department of Applied Information Sciences, Graduate School of Information Sciences, Tohoku University for a fruitful discussion.

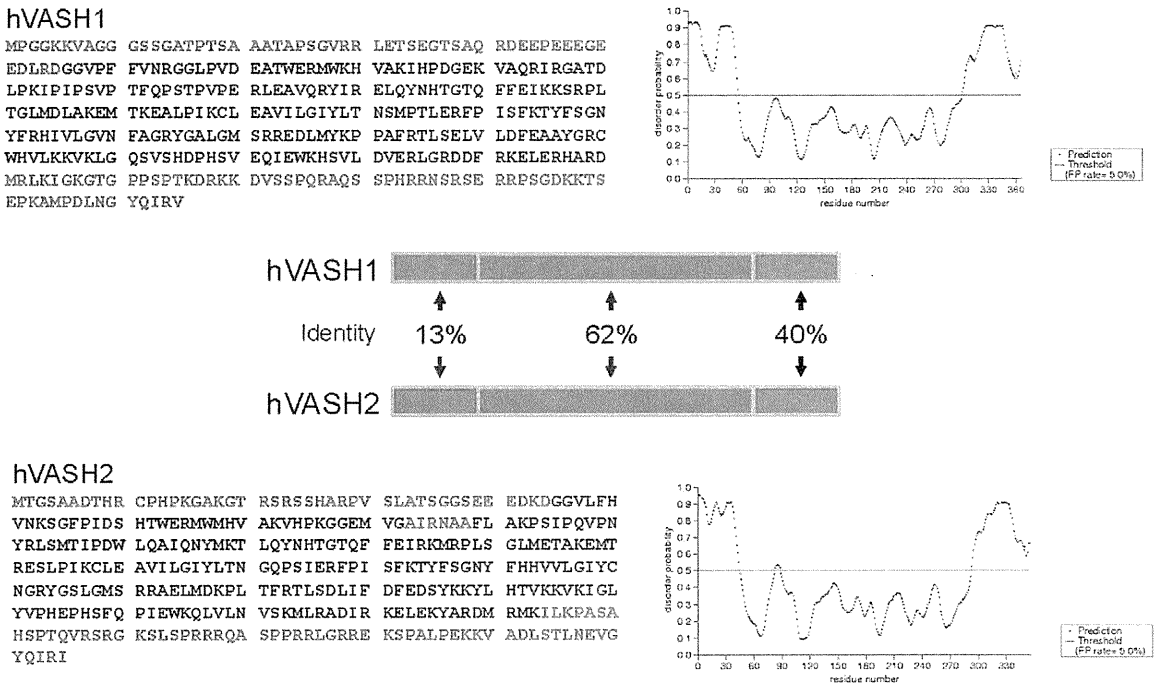

Fig. 5. Order/disorder configuration of human VASH1 and VASH2.Order/disorder configuration was determined by the Protein Disorder Prediction System (http://prdos.hgc.jp/cgi-bin/top.cgi). Amino acid sequences of human VASH1 and human VASH2 are shown on the left. Areas of red letters indicate disorder regions, whereas areas of black ones indicate the order region. The lines of disorder probability are shown graphically at the right. The similarity of order and disorder regions is indicated in the center.

References

Gerhardt, H., Betsholtz, C., 2003. Endothelial-pericyte interactions in angiogenesis. Cell Tissue Res. 314, 15–23.

Sato, Y., 2006. Update on endogenous inhibitors of angiogenesis. Endothelium 13, 147–155.

Abe, M., Sato, Y., 2001. cDNA microarray analysis of the gene expression profile of VEGF-induced human umbilical vein endothelial cells. Angiogenesis 4, 289–298.

Watanabe, K., et al., 2004. Vasohibin as an endothelium-derived negative feedback regulator of angiogenesis. J. Clin. Invest. 114, 898–907.

Shimizu, K., et al., 2005. Gene regulation of a novel angiogenesis inhibitor, vasohibin, in endothelial cells. Biochem. Biophys. Res. Commun. 327, 700–706.

Kern, J., et al., 2008. Alternative splicing of vasohibin-1 generates an inhibitor of endothelial cell proliferation, migration, and capillary tube formation. Arterioscler. Thromb. Vasc. Biol. 28, 478–484.

Shibuya, T., et al., 2006. Isolation and characterization of vasohibin-2 as a homologue of VEGF-inducible endothelium-derived angiogenesis inhibitor vasohibin. Arterioscler. Thromb. Vasc. Biol. 26, 1051–1057.

Nimmagadda, S., et al., 2007. Expression pattern of vasohibin during chick development. Dev. Dyn. 236, 1358–1362.

Naito, H., et al., 2009. Induction and expression of anti-angiogenic vasohibins in the hematopoietic stem/progenitor cell population. J. Biochem. 145, 653–659.

Yamashita, H., et al., 2006. Vasohibin prevents arterial neointimal formation through angiogenesis inhibition. Biochem. Biophys. Res. Commun. 345, 919–925.

Yoshinaga, K., et al., 2008. Expression of vasohibin as a novel endothelium-derived angiogenesis inhibitor in endometrial cancer. Cancer Sci. 99, 914–919.

Wakusawa, R., et al., 2008. Expression of vasohibin, an antiangiogenic factor, in human choroidal neovascular membranes. Am. J. Ophthalmol. 146, 235–243.

Tamaki, K., et al., 2008. Vasohibin-1 in human breast carcinoma: a potential negative feedback regulator of angiogenesis. Cancer Sci. 100, 88–94.

Sato, H., et al., 2009. Vitreous levels of vasohibin-1 and vascular endothelial growth factor in patients with proliferative diabetic retinopathy. Diabetologia 52, 359–361.

Hosaka, T., et al., 2009. Vasohibin-1 expressed in endothelium of tumor vessels regulates angiogenesis. Am. J. Pathol. 175, 430–439.

Miyake, K., et al., 2009. Inflammatory cytokine-induced expression of vasohibin-1 by rheumatoid synovial fibroblasts. Acta Med. Okayama. 63, 349–358.

Tamaki, K., et al., 2010. Vasohibin-1 as a potential predictor of aggressive behavior of ductal carcinoma in situ of the breast. Cancer Sci. 101, 1051–1058.

Yoshinaga, K., et al., 2011. Roles of intrinsic angiogenesis inhibitor, vasohibin, in cervical carcinomas. Cancer Sci. 102, 446–451.

Heishi, T., et al., 2010. Endogenous angiogenesis inhibitor vasohibin1 exhibits a broad-spectrum anti-lymphangiogenic activity and suppresses lymph node metastasis. Am. J. Pathol. 176, 1950–1958.

Kimura, H., et al., 2009. Distinctive localization and opposed roles of vasohibin-1 and vasohibin-2 in the regulation of angiogenesis. Blood. 113, 4810–4818.

Suzuki, Y., et al., 2010. Isolation of a small vasohibin-binding protein (SVBP) and its role in vasohibin secretion. J. Cell Sci. 123, 3094–4101.

Uversky, V.N., 2011. Intrinsically disordered proteins from A to Z. Int. J. Biochem. Cell Biol. 43, 1090–1103.

The EMBO Journal (2012) 31, 842–855 | © 2012 European Molecular Biology Organization | All Rights Reserved 0261-4189/12
www.embojournal.org

THE EMBO JOURNAL

Identification and characterization of a resident vascular stem/progenitor cell population in preexisting blood vessels

Hisamichi Naito[1], Hiroyasu Kidoya[1], Susumu Sakimoto[1], Taku Wakabayashi[1] and Nobuyuki Takakura[1,2,*]

[1]Department of Signal Transduction, Research Institute for Microbial Diseases, Osaka University, Osaka, Japan and [2]JST, CREST, Sanbancho, Tokyo, Japan

Vasculogenesis, the *in-situ* assembly of angioblast or endothelial progenitor cells (EPCs), may persist into adult life, contributing to new blood vessel formation. However, EPCs are scattered throughout newly developed blood vessels and cannot be solely responsible for vascularization. Here, we identify an endothelial progenitor/stem-like population located at the inner surface of preexisting blood vessels using the Hoechst method in which stem cell populations are identified as side populations. This population is dormant in the steady state but possesses colony-forming ability, produces large numbers of endothelial cells (ECs) and when transplanted into ischaemic lesions, restores blood flow completely and reconstitutes *de-novo* long-term surviving blood vessels. Moreover, although surface markers of this population are very similar to conventional ECs, and they reside in the capillary endothelium sub-population, the gene expression profile is completely different. Our results suggest that this heterogeneity of stem-like ECs will lead to the identification of new targets for vascular regeneration therapy.

The EMBO Journal (2012) **31,** 842–855. doi:10.1038/emboj.2011.465; Published online 16 December 2011
Subject Categories: development; molecular biology of disease
Keywords: angiogenesis; endothelium; side population; somatic stem cell

Introduction

Regeneration of the vasculature in ischaemic-injured organs is essential to ensure their integrity. Postnatal neovascular formation was originally thought to be mediated by angiogenesis, that is, the generation of new endothelial cells (ECs) from preexisting vessels, not by vasculogenesis, a process of blood vessel formation whereby the early vascular plexus forms from mesoderm by differentiation of angioblasts (Risau, 1997). However, accumulating evidence suggests that vasculogenesis persists into adult life, and contributes to the formation of new blood vessels (Asahara *et al*, 1997). It has been proposed that bone marrow (BM)-derived circulating endothelial progenitor cells (EPCs) are important for promoting vascularization in many pathophysiological situations; several clinical trials are already ongoing based on this concept (Shantsila *et al*, 2007). However, some reports suggest that the contribution of EPCs to the neovascular ECs itself is not sufficient (Gothert *et al*, 2004; Peters *et al*, 2005).

In the peripheral vasculature, there is considerable evidence that although preexisting ECs display many common features, they also represent a heterogeneous population. Transcriptional and antigenic differences in ECs from arteries and veins, and the morphological and functional characteristics referred to as continuous, fenestrated, and discontinuous are widely accepted (Risau, 1995). Recently, it has been shown that in response to angiogenic stimuli, a discrete population of cells, the so-called 'tip and stalk cells', lead and guide new sprouts and form additional ECs, respectively (Gerhardt *et al*, 2003). Furthermore, populations of ECs of another different phenotype, the so-called phalanx cells that generate stable blood vessels, have been reported (Mazzone *et al*, 2009).

Additionally, the presence of stem/progenitor cells in the vessel wall has been proposed. Investigating adult vessels in mice revealed $Sca1^+$ progenitor cells in the adventitia of large and medium-sized arteries and veins (Hu *et al*, 2004; Sainz *et al*, 2006; Passman *et al*, 2008). Similarly, $CD34^+$ $CD31^-$ progenitor cells in the distinct zone between smooth muscle and the adventitial layer of the human adult vascular wall were identified (Zengin *et al*, 2006). These stem/progenitor cells were reported to have the ability to differentiate into ECs in culture and form capillary-like microvessels in *ex-vivo* assays. However, during angiogenic growth, microvascular ECs, rather than the ECs of the artery or vein which are completely covered by the vascular wall, are selected for neovascularization (Risau, 1995). Therefore, it is suggested that stem/progenitor cells in the vascular wall of larger blood vessels are not the main source of neovascular ECs.

Haematopoietic cells (HCs) and ECs originate from common progenitors (Choi *et al*, 1998), with haemogenic ECs generating HCs during development (Nishikawa *et al*, 1998). Moreover, ECs support self-renewal of haematopoietic stem cells (HSCs; Hooper *et al*, 2009). We previously reported that HSCs also promote angiogenesis (Takakura *et al*, 2000), emphasizing the close developmental and functional relationships between HCs and ECs. Most BM HSCs appear dormant, and are characterized as side population (SP) cells effluxing Hoechst 33342 (Goodell *et al*, 1996). This staining method has been applied to explore stem cells of a wide range of tissues, including skin, lung, heart, mammary gland, muscle and testis (Challen and Little, 2006). It is possible that resident quiescent EC stem/progenitor cells in the preexisting blood vessels are also found within these SP cells. In this

*Corresponding author. Department of Signal Transduction, Research Institute for Microbial Diseases, Osaka University, 3-1 Yamada-oka, Suita, Osaka 565-0871, Japan. Tel.: +81 6 6879 8312; Fax: +81 6 6879 8314; E-mail: ntakaku@biken.osaka-u.ac.jp

Received: 5 June 2011; accepted: 23 November 2011; published online: 16 December 2011

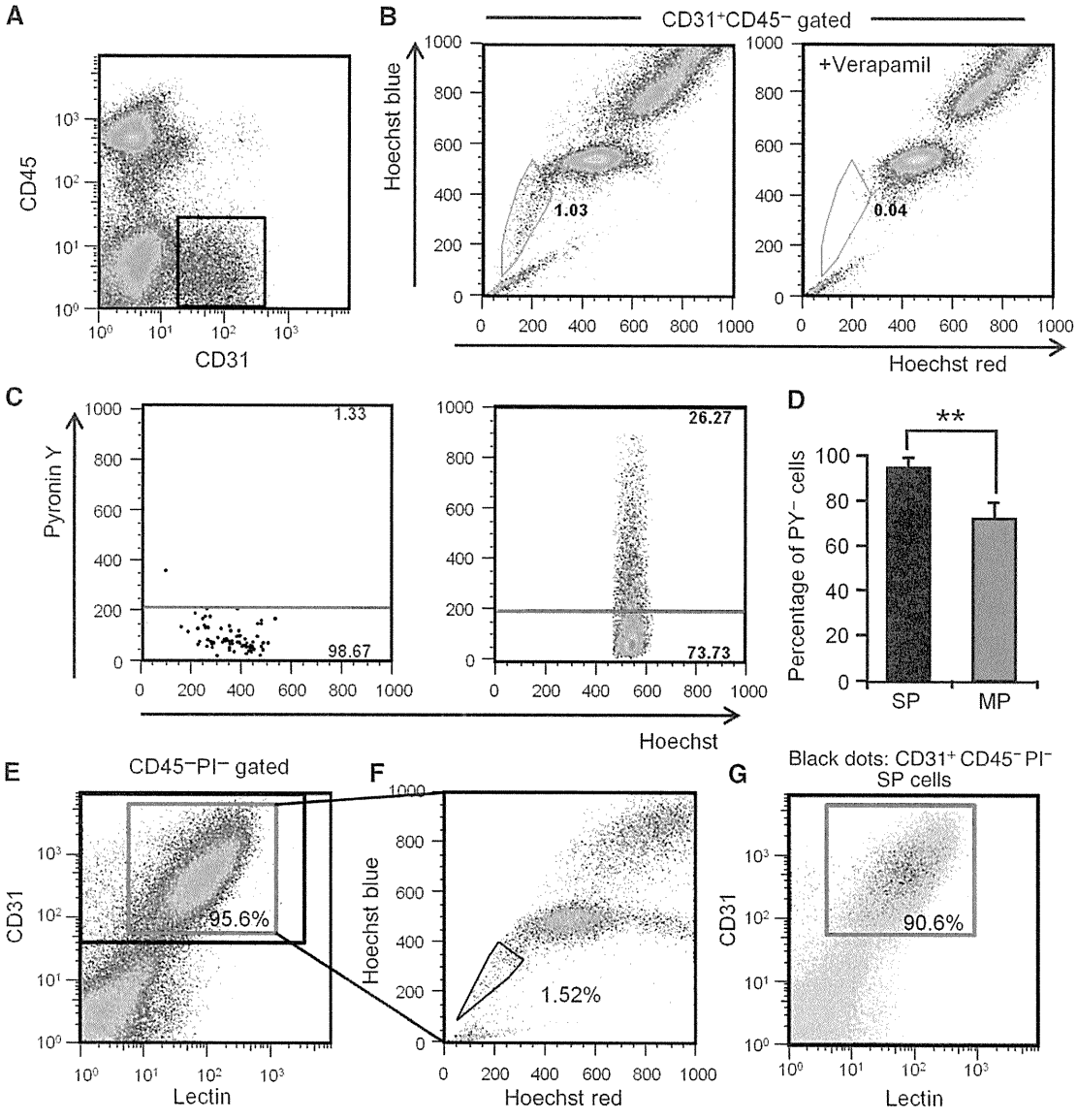

Figure 1 Identification of endothelial side population cells. (**A**) Flow cytometric analysis of hind limb ECs from wild-type mice. (**B**) Hoechst 33342 staining of $CD31^+CD45^-$ ECs gated as shown in (**A**). Note that verapamil selectively prevents Hoechst exclusion from EC-SP cells. (**C**) Incorporation of Pyronin Y (PY) in EC-SP (left-hand side) and EC-MP (right-hand side) cells. (**D**) Quantitative evaluation of PY^- cells among EC-SP (SP) and EC-MP (MP) cells. Error bars are ± s.e.m. $^{**}P<0.01$ ($n=7$). (**E**) Flow cytometric analysis of mouse hind limb ECs after *in-vivo* infusion of lectin. Lectin-positive cells among the $CD31^+CD45^-$ cells are shown in the red gate and total $CD31^+CD45^-$ cells are shown in the black gate. 95.9 ± 0.2% ($n=6$) of the $CD31^+CD45^-$ ECs were lectin positive. (**F**) Hoechst staining of $lectin^+$ $CD31^+CD45^-$ cells. (**G**) Representative flow cytometric plots of EC-SP cells (black dots). The lectin-positive population is shown in the red gate. 90.6 ± 1.4% ($n=4$) of the EC-SP cells were lectin positive.

study, we examined the ECs residing in preexisting vessels precisely to identify the origin of neovascular ECs.

Results

Identification and characterization of endothelial SP cells

Here, we analysed cells from hind limb muscle to identify endothelial SP cells. Among cells stained by the EC marker CD31, but not the HC marker, CD45 ($CD31^+$ $CD45^-$ ECs) (Figure 1A), 1.15 ± 0.14% were in the SP gate, confirmed by their disappearance with the drug efflux pump inhibitor, verapamil. They were distinct from the main population (MP) of cells (Figure 1B). Because the SP phenotype is a marker for quiescence in HSCs (Arai *et al*, 2004), we applied a method which identifies cells in G0 plus G1 phase by Hoechst 33342 distribution and assigns them to G0 or G1 by Pyronin Y RNA staining (Gothot *et al*, 1997). As shown in Figure 1C and D, 94.8 ± 2.2% of endothelial SP (EC-SP) cells were in the PY^- G0 fraction, clearly different from $CD31^+CD45^-$ endothelial MP (EC-MP) cells. To confirm that EC-SP cells do reside in the blood vessel, we performed lectin perfusion assays. As shown in Figure 1E, ~96% of $CD31^+CD45^-$ cells were lectin positive, indicating that most of them were true ECs residing at the inner surface of vessels. The percentage of SP cells within the $lectin^+$ EC population was approximately the same as the percentage of EC-SP cells identified in Figure 1B (see Figure 1F). On the other hand, ~91% of EC-SP cells were $lectin^+$, indicating that most of these cells reside at the inner surface of vessels (Figure 1G). Next, we

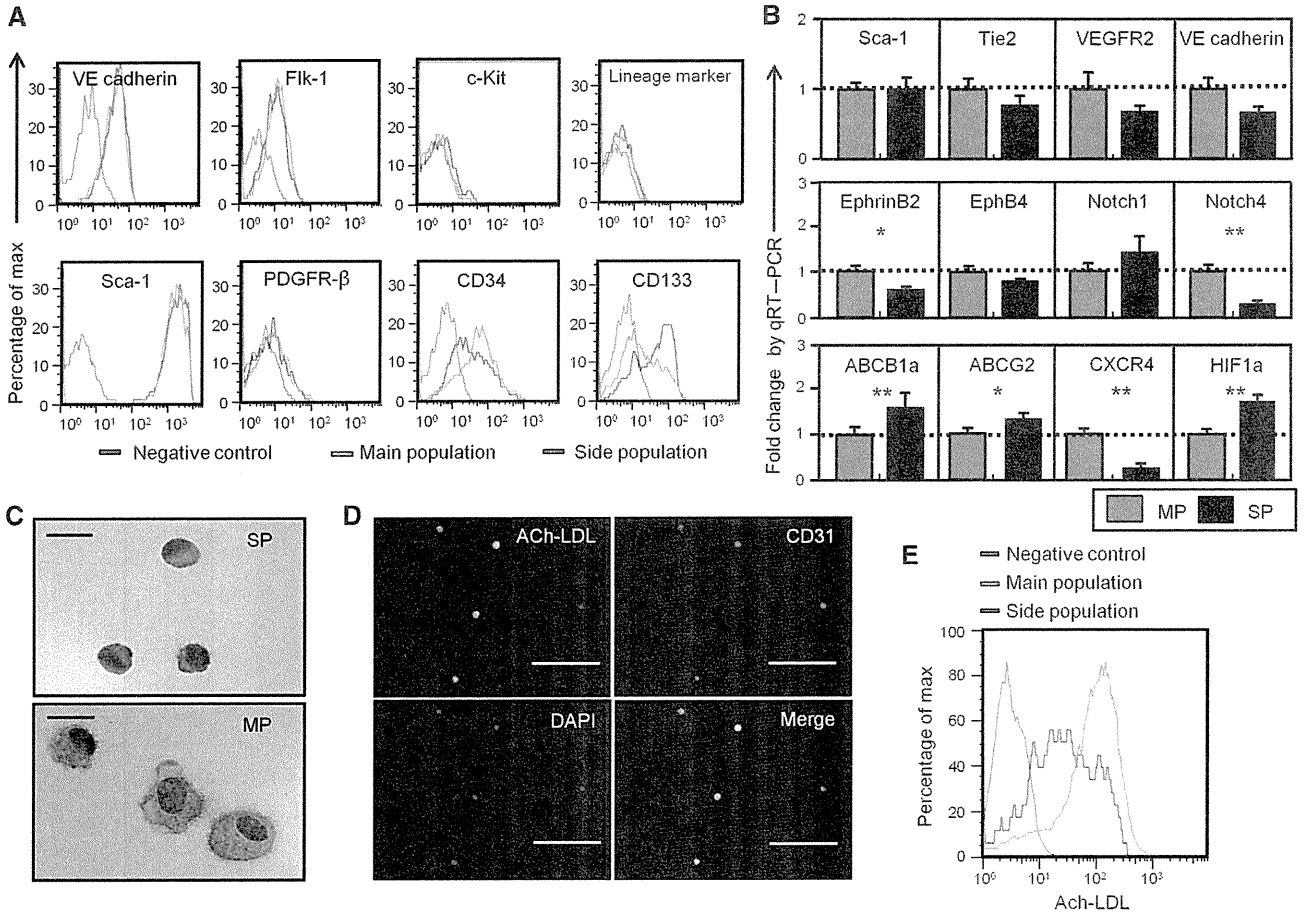

Figure 2 Characterization of endothelial side population cells. (**A**) Histogram showing expression levels of surface markers in EC-SP, EC-MP cells and the negative control. (**B**) Quantitative RT–PCR analysis of mRNA as indicated in EC-SP and EC-MP cells, corrected for expression of the control gene GAPDH. Of the endothelial genes, Notch4 was significantly lower in EC-SP cells. Expression levels of the ABC transporter ABCG2 and ABCB1a (MDR1a) were higher in EC-SP cells. Expression of chemokine receptor CXCR4 and hypoxia-inducible factor (HIF1a) was higher in EC-SP cells. Error bars are ±s.e.m. $^{**}P<0.01$, $^{*}P<0.05$ ($n>6$). (**C**) Haematoxylin and eosin staining of EC-SP and EC-MP cells isolated by FACS. (**D**) Freshly isolated cells from hind limb were stained with Ac-LDL and then Hoechst staining was performed to detect EC-SP cells. EC-SP cells were cytospun onto slides and Ac-LDL uptake was evaluated. Some of the EC-SP cells showed weak uptake of Ac-LDL, but all were positive. (**E**) Intensity of Ac-LDL uptake was evaluated by FACS analysis. As indicated, Ac-LDL uptake was observed in EC-SP cells but was lower than in EC-MP cells. Scale bars, 10 μm (**C**) and 100 μm (**D**).

characterized the phenotype of EC-SP cells. These were found to express the EC markers VE-cadherin, Flk-1, and Sca-1, but no haematopoietic lineage markers or the pericyte marker PDGFR-β. This phenotype is identical to the EC-MP cells. However, as with CD34-negative long-term repopulating HSCs (Osawa *et al*, 1996), EC-SP cells expressed little CD34, but CD133, a stem/progenitor cell marker in several tissues (Mizrak *et al*, 2008), was strongly expressed (Figure 2A). We confirmed that the EC-SP cell fraction was not contaminated with HCs, pericytes, or fibroblasts, by analysing lineage markers for those cell types in cells from the digested muscle sample (Supplementary Figures S1 and S2). Moreover, Notch4 mRNA levels were significantly lower in EC-SP than in EC-MP cells. In contrast, mRNA expression for ABCB1a (Multiple drug resistance 1a (MDR1a)) and ABCG2, a member of the ABC transporter gene family correlating with SP phenotype (Bunting *et al*, 2000), was higher in the EC-SP cells (Figure 2B). Furthermore, the expression of several other ABC transporters that are reported to correlate with SP phenotype was higher in the EC-SP cells (Supplementary Figure S3). Morphologically, the nuclear-to-cytoplasm (N/C) ratio of the EC-SP cells was higher than the EC-MP cells (Figure 2C). In addition, acetylated low-density lipoprotein (Ac-LDL) uptake that is functional property of ECs was observed by EC-SP cells but less than by EC-MP cells (Figure 2D and E). Taken together, we conclude that EC-SP cells are not pericytes, fibroblasts, or HCs but are true ECs already committed to the EC lineage and are phenotypically and morphologically different from EC-MP cells.

EC-SP cells are not derived from BM, are distinct from EPCs, and are distributed in the peripheral vessels

To exclude the possibility that EC-SP cells are only found in the lower limb, we analysed different organs and confirmed that these cells are distributed all over the body, but are not detectable in some organs (Figure 3A–C). For example, we could not identify the EC-SP pattern in the brain, probably due to constitutively high ABC transporter expression (Miller, 2010; Figure 3A and C). In addition, we were unable to detect the SP pattern in cultured ECs (Figure 3A and C). Interestingly, EC-SP cells were also not detectable in peripheral blood or BM, suggesting an origin different from EPCs

A

	Percentage of EC-SP cells		Percentage of EC-SP cells
Lung	0.96±0.09	bEnd3	Undetectable
Liver	1.47±0.15	EOMA	Undetectable
Hindlimb muscle	1.15±0.11	HUAEC(P=4)	Undetectable
Heart	1.55±0.14	HUVEC(P=4)	Undetectable
Bone marrow	Undetectable	Mouse EC (P=4)	Undetectable
Peripheral blood	Undetectable	Brain	Hoechst method did not work

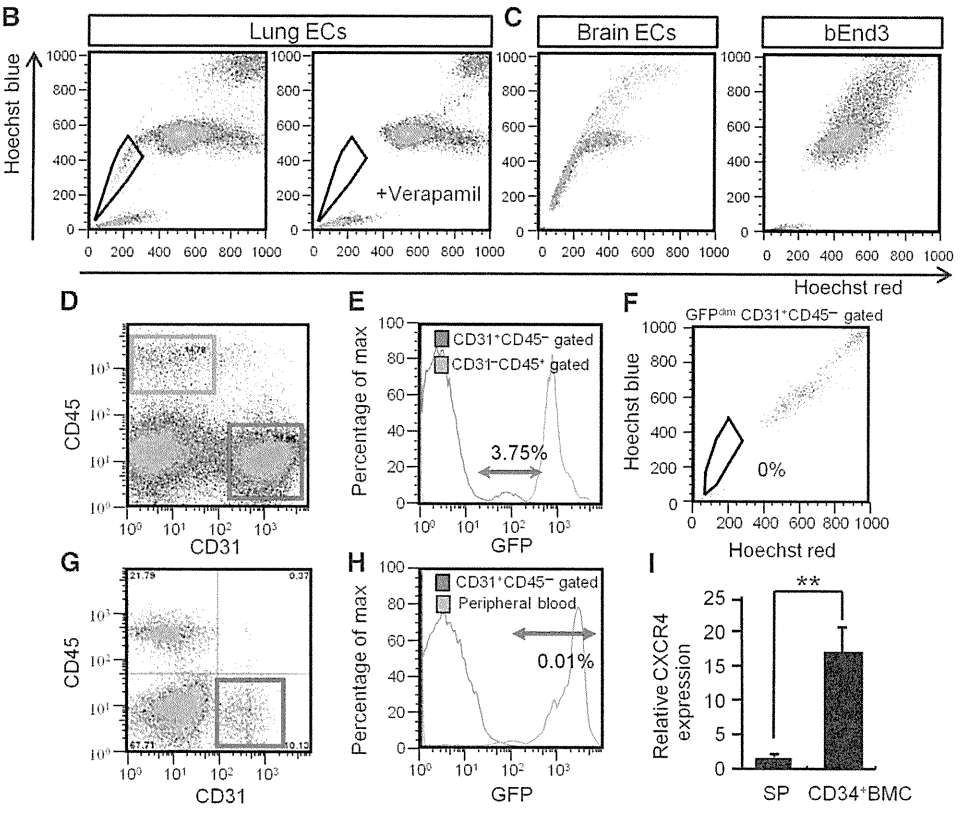

Figure 3 EC-SP cells are present in different organs and are not derived from BM in BM chimeric mice. (**A**) The ECs from several organs and cultured cell lines as indicated were stained with Hoechst. Percentages of the EC-SP cells are shown in the table. There were few $CD31^+CD45^-$ ECs in the bone marrow and peripheral blood; SP cells were hardly detected at all. In the EC lines (HUVEC, HUAEC, bEnd3, and EOMA), SP cells were not detected. Of note, the EC-SP phenotype disappeared after culturing primary ECs from hind limbs. (**B**) One example showing EC-SP cells of lung that disappeared following verapamil treatment. (**C**) In the brain, a stereotypic EC-SP pattern is not observed and there are no EC-SP cells within the bEnd3 population. (**D–F**) BM cells from GFP mice were transplanted into lethally irradiated wild-type mice. Four weeks after transplantation, cells from hind limbs were analysed. (**D**) Representative flow cytometric plots of cells from hind limb muscle. $CD31^+CD45^-$ EC fraction (red) and $CD31^-CD45^+$ peripheral blood fraction (green) are gated. (**E**) Histogram of $CD31^+CD45^-$ ECs and $CD31^-CD45^+$ peripheral blood cells obtained from hind limbs. Almost all blood cells (green line) after transplantation were GFP positive. Approximately 4% of $CD31^+CD45^-$ ECs (red line) were weakly GFP positive (GFP^{dim}). GFP^{dim} EC population is shown in arrowed region. (**F**) Hoechst staining of GFP^{dim} ECs. The SP phenotype was not seen. (**G, H**) Analysis of hind limb muscle cells from newborn transplantation model. (**G**) Representative flow cytometric plots of cells from hind limb muscle of BM chimeric mice; $CD31^+CD45^-$ EC fraction is gated (red). (**H**) Histogram showing GFP intensity of $CD31^+CD45^-$ ECs obtained from hind limb and peripheral blood. In this model, GFP-positive $CD31^+CD45^-$ ECs make up $<0.01\%$ of total $CD31^+CD45^-$ ECs, suggesting no major contribution of BM cells to EC-SP cells. (**I**) Quantitative evaluation of CXCR4 mRNA expression in EC-SP cells and $CD34^+$ bone marrow mononuclear cells (BMCs) by real-time PCR. Note that CXCR4 expression is 17 times higher in $CD34^+$ BM cells (BMC) than in EC-SP cells (SP). Error bars are ±s.e.m. $^{**}P<0.01$ ($n=7$).

and that EC-SP cells are present in the peripheral blood vessels. Moreover, EC-SP cells are not present in the lymphatic endothelium (Supplementary Figure S4) and express lower levels of arterial markers but similar levels of venous markers compared with total ECs (Supplementary Figure S5). This indicates that EC-SP cells reside predominantly in veins and capillaries but not in the lymphatics. To confirm that EC-SP cells are not identical to EPCs, we transplanted BM cells from GFP mice into irradiated wild-type mice and assessed the presence of GFP-positive EC-SP cells. Flow cytometry showed that among $CD31^+CD45^-$ ECs from the hind limb muscle of GFP BM-transplanted mice (Figure 3D), 3.75±0.13% were GFP^{dim} (Figure 3E), but that none of these were EC-SP cells (Figure 3F). This was also confirmed in a BM transplantation model using neonates, in which BM cells were replaced by the injection of BM cells from GFP mice into the liver of wild-type neonates within 12 h after birth. This model allows us to ask whether EPCs derived from BM undergo EC transition at the growing stage and become EC-SP cells. However, among $CD31^+CD45^-$ ECs from the hind limb muscle of GFP newborn BM-transplanted mice (Figure 3G), we could not detect any GFP-positive or GFP-dim

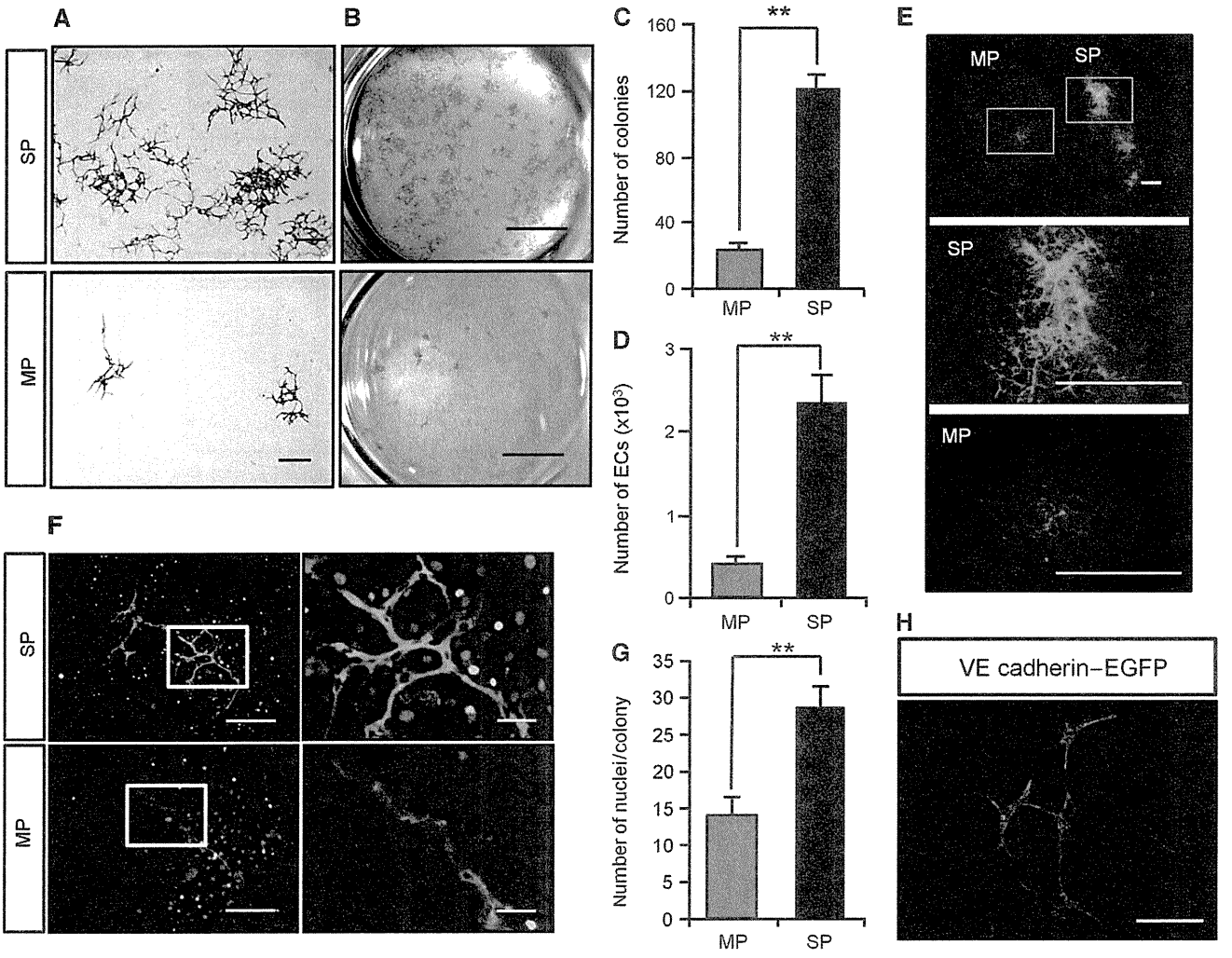

Figure 4 Endothelial SP cells have EC colony-forming ability. (**A**) EC-SP cells and EC-MP cells were cultured on OP9 feeder cells and stained with anti-CD31 antibody. (**B**) Colonies are shown in the low power field. The EC-SP cells form fine CD31-positive networks and many colonies compared with EC-MP cells. (**C**) The number of colonies stained with anti-CD31 antibody and (**D**) number of VE-cadherin$^+$ ECs counted by flow cytometry in one well of a 6-well culture dish. Error bars are ± s.e.m. $^{**}P<0.01$ ($n=12$). (**E**) EC-SP and EC-MP cells were sorted from EGFP mice and transplanted to wild-type mice with matrigel. Gated area is shown in higher magnification. (**F**, **G**) Nuclear staining of ECs forming colonies on OP9 cells for the evaluation of cell number. Representative image of an EC colony stained with anti-CD31 antibody and Hoechst (**F**) and quantification of the number of ECs composing one colony (**G**). (**H**) EC colonies derived from EC-SP cells from VE-cadherin promoter EGFP mice. Scale bars, 500 μm (**A**), 1 mm (**E**), 200 μm (**F** left panel and **H**), 50 μm (**F** right panel), and 5 mm (**B**).

ECs, suggesting that EC-SP cells do not originate from EPCs derived from BM (Figure 3H). It has been reported that EPCs express CXCR4 (Walter *et al*, 2005); accordingly, the BM CD34$^+$ EPC cell fraction strongly expresses CXCR4. However, EC-SP cells were found to express CXCR4 at significantly lower levels (Figure 3I). Taking these data together, we conclude that EC-SP cells are not identical to EPCs.

Proliferation and colony-forming capacity of EC-SP cells in vitro

If EC-SP cells are indeed a stem/progenitor population, they must be able to generate large numbers of mature ECs and form colonies originating from a single EC. To explore this issue *in vitro*, sorted EC-SP cells were cultured on OP9 stromal cells which support EC growth (Takakura *et al*, 1998). After 10 days, EC-SP cells generated higher numbers of colonies with a 'cordlike' structure (Zhang *et al*, 2001), which formed a fine vascular network, as well as producing higher numbers of ECs than EC-MP cells (Figure 4A–D). It was estimated that 1.2 ± 0.5% of EC-SP cells formed cobblestone-like (sheet-like) colonies (Supplementary Figure S6). To ensure that this degree of colony-forming ability was not a specific property only of ECs from hind limb muscle vessels, EC-SP cells from different organs were cultured on OP9 stromal cells. It was found that they also possessed greater colony-forming ability than EC-MP cells (Supplementary Figure S7). Moreover, we confirmed that these colony-forming cells are indeed ECs, because the colonies were positive for the EC markers CD34, CD105, Flk1, VE-cadherin, vWF, and ZO-1 (Supplementary Figure S8) but negative for the haematopoietic markers B220, CD4, CD8, Gr1, Mac1, Ter119, and CD45 (Supplementary Figure S9A). We excluded the possibility that a contaminating HSC population was giving rise to ECs in our culture system by demonstrating that CD31$^+$ ECs could not be induced from BM-derived c-Kit$^+$Sca-1$^+$Lin$^-$ HSC populations (Supplementary Figure S9B). Moreover, VEGF blockade resulted in prevention of colony formation, indicating that expansion of ECs from

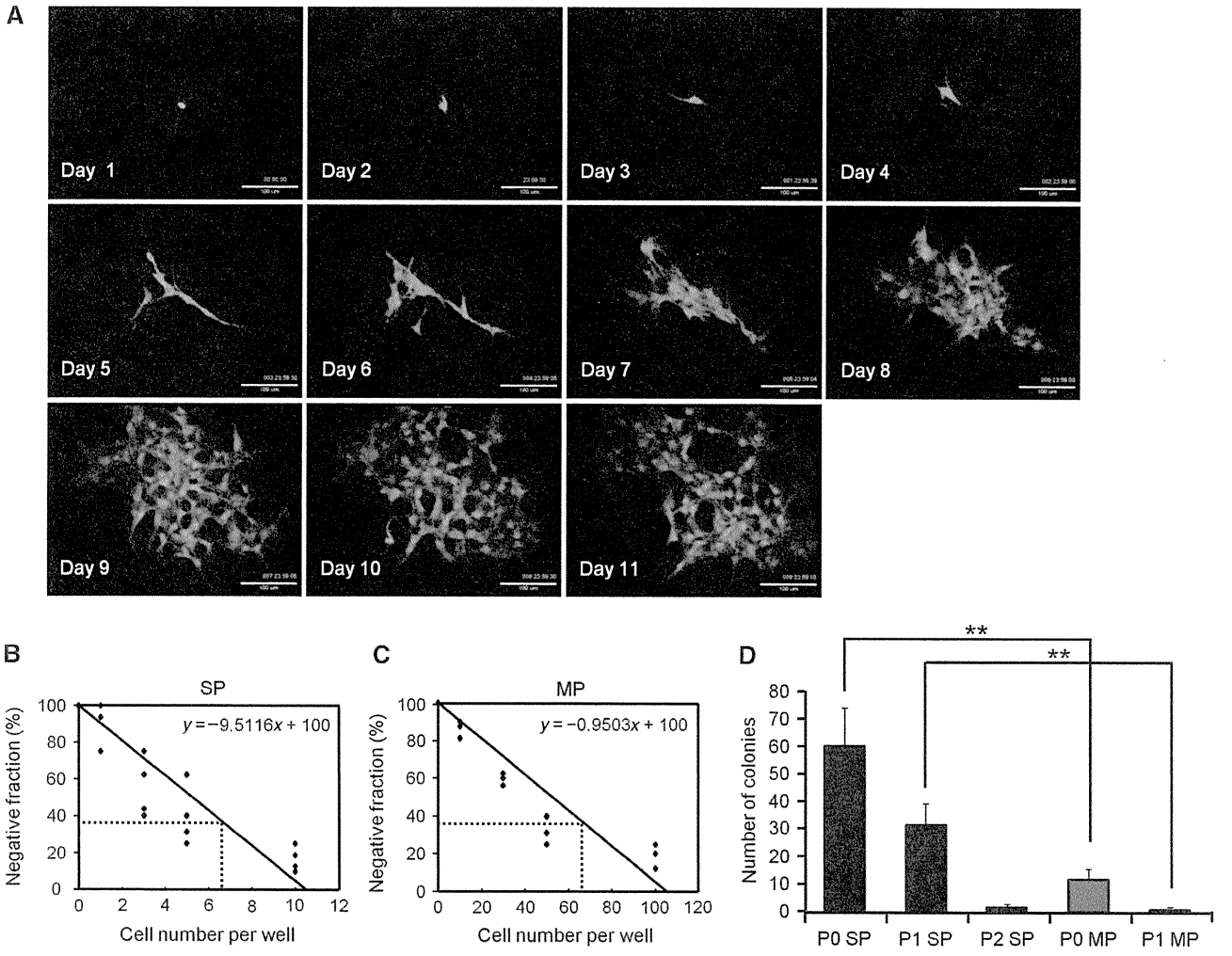

Figure 5 Single EC-SP cells form EC colonies. (**A**) Time-lapse analysis of EC-SP cell from EGFP mice. (**B**, **C**) Limiting dilution assay of EC-SP (**B**) and EC-MP (**C**) cells. EC-SP and EC-MP cells were cultured on OP9 feeder cells and titrated down to 20, 10, 5, 3, 1, 0 and 200, 100, 50, 30, 10, 0 cells, respectively. The number of colonies was counted after staining with anti-CD31 antibody and the frequency of colony-forming cells was calculated according to Poisson statistics. (**D**) Results of long-term culture-initiating assays. 5×10^2 primary EC-SP or EC-MP cells were cultured and the number of colonies counted (P0). Cells were harvested and 5×10^2 sorted ECs derived from the first or second rounds of culture were cultured again (P1 and P2, respectively). Note that the P2 assay using ECs from EC-MP cells could not be performed due to insufficient ECs in P1. $^{**}P<0.01$ ($n>5$). Scale bar, 100 μm (**A**).

EC-SP cells depended on VEGF-VEGFR signalling (Supplementary Figure S10). Matrigel plug assays carried out with GFP-positive cells showed that EC-SP cells formed entire vascular networks in the matrigel, but EC-MP cells only formed separate colonies with a small network (Figure 4E). Moreover, to compare the ability of single EC-SP or EC-MP cells to generate EC, numbers of cells in single colonies were counted. It was found that EC-SP cells have a greater capacity to produce ECs than do EC-MP cells (Figure 4F and G). To further clarify whether EC-SP cells are indeed committed to the EC lineage, we crossed endothelial-specific VE-cadherin-Cre-ERT mice with loxP-CAT-EGFP reporter mice and sorted GFP-positive EC-SP cells (Supplementary Figure S11A and B). In the GFP^+ ($VE\text{-}cadherin^+$) $CD31^+CD45^-$ fraction, the percentage of EC-SP cells was comparable to wild-type mice. When cultured on OP9 cells for 10 days, GFP^+ EC-SP cells generated colonies similar to those from wild-type mice (Figure 4H). Furthermore, EC-SP cells did not give rise to the mesenchymal and haematopoietic lineage *in vitro* (Supplementary Figures S12 and S13A). Next, to assess clonal expansion of ECs from single cells, we performed time-lapse analysis of EC-SP cells and found that a single EC-SP cell could form a colony (Figure 5A; Supplementary Movie S1). Moreover, to establish whether this EC-SP cell clonal expansion can occur in every colony, sorted EC-SP cells from normal mice and C57BL/6-Tg(CAG-EGFP) mice (EGFP mice) were mixed in equal proportions and cultured on OP9 stromal cells. As expected, colonies with 'cordlike' structures were generated from either GFP-positive or -negative ECs (Supplementary Figure S14), suggesting that a single EC-SP cell is able to generate a single colony. Limiting dilution analysis revealed that the frequency of cells with the capacity to form colonies was significantly higher in EC-SP cells than in EC-MP cells by a factor of 10 (1 in 6.6 and 1 in 66, respectively) (Figure 5B and C). Moreover, long-term culture-initiating cell (LTC-IC) assays revealed that ECs having higher proliferative potential were produced from EC-SP cells than could be produced by EC-MP cells (Figure 5D). These findings indicate that cells able to generate EC colonies are enriched within the EC-SP population.